Survival of flux transfer event (FTE) flux ropes far along the tail magnetopause

J. P. Eastwood,[1] T. D. Phan,[2] R. C. Fear,[3] D. G. Sibeck,[4] V. Angelopoulos,[5] M. Øieroset,[2] and M. A. Shay[6]

Received 13 March 2012; revised 2 July 2012; accepted 8 July 2012; published 23 August 2012.

[1] During intervals of southward IMF, magnetic reconnection can result in the formation of flux transfer events (FTEs) on the dayside magnetopause which travel along the magnetopause in the anti-sunward direction. Of particular interest is their fate and the role they play transporting solar wind plasma into the magnetosphere. We present the discovery of FTEs far along the distant tail magnetopause (x = −67 Earth radii) using data from ARTEMIS on the dusk flank magnetopause under southward/duskward IMF conditions. The identification of several events is further supported by excellent fits to a force-free flux rope model. The axis of each structure is principally north-south, i.e., perpendicular to the Sun-Earth line. Simultaneous observations by THEMIS on the dayside magnetopause indicate that FTEs are being produced there, although perhaps 2–4 times smaller in size. The convection time from the dayside magnetopause to ARTEMIS is 30 min, and the FTEs have a flux content comparable to those typically observed on the dayside magnetopause, indicating that these features are in quasi-equilibrium as they are convected downtail. By considering the relative orientations of the FTEs observed by THEMIS and ARTEMIS, the magnetic field geometry is consistent with the FTEs being produced on the dayside magnetopause along an extended X-line in the presence of IMF B_y and bending as they are convected to the flanks.

Citation: Eastwood, J. P., T. D. Phan, R. C. Fear, D. G. Sibeck, V. Angelopoulos, M. Øieroset, and M. A. Shay (2012), Survival of flux transfer event (FTE) flux ropes far along the tail magnetopause, *J. Geophys. Res.*, *117*, A08222, doi:10.1029/2012JA017722.

1. Introduction

[2] At Earth, the solar wind–magnetosphere interaction is chiefly governed by the orientation of the interplanetary magnetic field (IMF) as it impinges on the dayside magnetosphere. In particular, if the IMF points southward (i.e., $B_z < 0$ in the Geocentric Solar Magnetospheric (GSM) coordinate system), then subsolar magnetopause reconnection leads to plasma entry and the so-called 'open magnetosphere' [*Dungey*, 1961; *Fairfield and Cahill*, 1966], with plasma added to the magnetotail plasma sheet via reconnection in the magnetotail.

[3] This basic picture implies that the transport of reconnected plasma into the magnetotail is steady and smooth. However, experimental evidence and computer simulations suggest that even under relatively steady solar wind conditions magnetopause reconnection can be unsteady and/or multipoint in nature, leading to the formation of flux transfer events (FTEs) which are observed on the magnetopause [*Russell and Elphic*, 1978; *Raeder*, 2006; *Omidi and Sibeck*, 2007; *Fear et al.*, 2008; *Hasegawa et al.*, 2010; *Øieroset et al.*, 2011]. Various formation mechanisms have been proposed based on patchy reconnection [*Russell and Elphic*, 1978], bursty reconnection at a single elongated X-line [*Southwood et al.*, 1988; *Scholer*, 1988] and multiple X-line reconnection [*Lee and Fu*, 1985].

[4] The vast majority of FTE observations have been made on the dayside magnetopause and to distances of ~10 R_E downtail [*Kawano and Russell*, 1997; *Fear et al.*, 2005; *Wang et al.*, 2006; *Dunlop et al.*, 2011a, 2011b], and so the evolution and fate of FTEs as they are transported into the magnetotail is poorly understood. It has been proposed that if they form as flux tubes in the manner described by *Russell and Elphic* [1978] then their axes should rotate toward orientations parallel to the Sun-Earth line, and 'sink' into the magnetospheric lobe [*Sibeck and Siscoe*, 1984]. However, if FTEs are formed by multiple X-line reconnection, they may become connected to the ionosphere at both

[1]Blackett Laboratory, Imperial College London, London, UK.
[2]Space Sciences Laboratory, University of California, Berkeley, California, USA.
[3]Department of Physics and Astronomy, University of Leicester, Leicester, UK.
[4]NASA Goddard Space Flight Center, Greenbelt, Maryland, USA.
[5]Institute of Geophysics and Planetary Physics, University of California, Los Angeles, California, USA.
[6]Department of Physics and Astronomy, Bartol Research Institute, University of Delaware, Newark, Delaware, USA.

Corresponding author: J. P. Eastwood, Blackett Laboratory, Imperial College London, Prince Consort Road, London SW7 2AZ, UK. (jonathan.eastwood@imperial.ac.uk)

0148-0227/12/2012JA017722

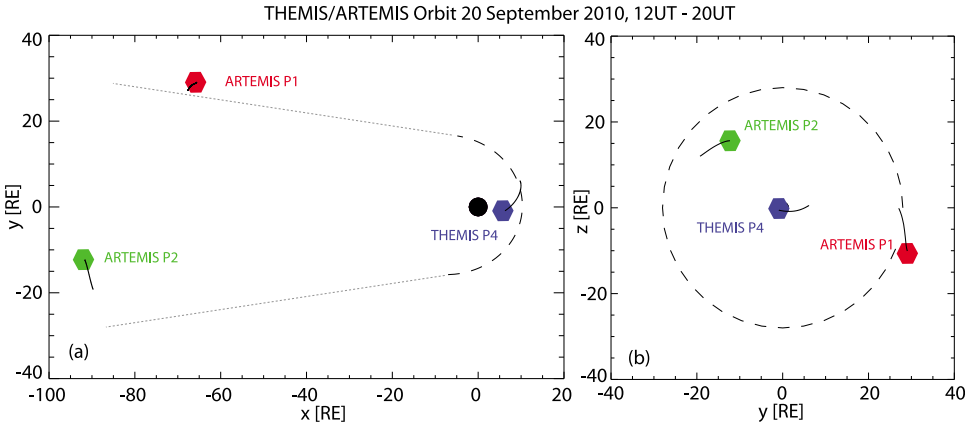

Figure 1. (a) Satellite orbit plot in the x-y GSM plane between 12:00 UT and 20:00 UT on 20 September 2010. (b) Plot in the y-z GSM plane. The symbols indicate the location of each probe at the start of the interval. The dashed line represents the model magnetopause, calculated according to the *Farris et al.* [1991] model with appropriate solar wind conditions (n = 8 cm^{-3}, v = 330 km s^{-1}). In the absence of an appropriate tail magnetopause model, the dotted line is a linear extension to ARTEMIS P1. In Figure 1b, the circle has radius 28 Re, corresponding to the location of the magnetopause at the x location of ARTEMIS P1.

ends, or open to the solar wind at both ends [*Lee and Fu*, 1985], in which case the term flux transfer event would be a misnomer, since in the latter case these structures would not transfer magnetic flux into the magnetotail.

[5] THEMIS and ARTEMIS [*Angelopoulos*, 2008, 2011; *Sibeck et al.*, 2011] provide a new opportunity to examine global solar wind entry modes, by making simultaneous subsolar and distant flank observations for the first time. Here we present new observations from ARTEMIS showing the survival of FTE flux ropes far along the tail magnetopause at x = −67 R_E on the dusk flank, with flux content similar to that of FTEs at the dayside. These measurements are complemented by simultaneous THEMIS measurements of the dayside magnetopause and observations of FTEs there.

2. Overview of the Observations

[6] THEMIS initially consisted of five identical satellites, or probes, placed in orbit around the Earth to study the physics of substorms. In 2009, two of the probes (P1 and P2) were removed from the THEMIS constellation to form ARTEMIS, and in mid-2011 were finally placed in lunar orbit, following nine months when the probes were located at the Earth–Moon Lagrange points. The present observations were made after P1 had been inserted into a Lissajous orbit around the L2 Lagrange point (P2 was still in a translunar orbit, approaching its own Lissajous orbit insertion at the L1 Lagrange point).

[7] On 20 September 2010 the THEMIS and ARTEMIS satellites were simultaneously observing both the dayside magnetosphere and the flanks of the magnetosphere (Figure 1a). ARTEMIS P1 was on the dusk flank of the magnetosphere at x = −65 R_E (the dotted line shows a simple straight-line extrapolation of the magnetopause from the *Farris et al.* [1991] model) while THEMIS P4 crossed the dayside magnetopause near the nose of the magnetosphere. ARTEMIS P2 was on the dawn flank of the magnetosphere at x = −90 R_E, but is not discussed further because it did not observe the magnetopause during the interval to be considered. Figure 1b shows the satellite locations projected into the y-z GSM plane. The dashed circle represents an estimated magnetopause at the x-location of ARTEMIS P1.

[8] Figure 2 shows an overview of the data. The upstream solar wind magnetic field, measured by Wind, is shown in Figures 2a–2c. Based on an inter-comparison of Wind and THEMIS P4 data in the magnetosheath, the Wind data has been lagged by 87 min so that it corresponds to the conditions at the nose of the magnetosphere. The magnetic field, initially northward, turned southward and duskward ($B_y > 0$) at ∼17:30 UT. Based on the location of P1 and the measured magnetosheath flow speed (∼300 km s^{-1}), it took approximately 27 min for the shocked solar wind, and the associated frozen-in IMF orientation, to flow from the nose of the magnetosphere (∼x = 10 R_E) to the flanks where P1 was situated. This advection time is confirmed by the later northward turning in B_z which occurred at ∼19:30 UT at P4 and ∼20:00 UT at P1 (at the end of the interval shown in Figure 2).

3. ARTEMIS P1 Dusk Flank Magnetopause Observations

[9] At 18:00 UT, P1 was located in the magnetosheath (v_X ∼ −300 km s^{-1} in Figure 2e), and subsequently encountered the magnetospheric plasma sheet three times (marked by blue bars in Figure 2d, characterized by stagnating flow and $B_z > 0$). Identification of the distant tail magnetopause can be difficult because the magnetosheath Alfvén speed is low and plasma properties can change very little across the magnetopause [*Hasegawa et al.*, 2002a, 2002b]. Around 18:02 UT and 18:14 UT, the flow speed decreases somewhat and the magnetic field points Earthward ($B_x > 0$). We identify this as the mantle, where relatively fast flowing plasma is contained on field lines of magnetospheric configuration [*Maezawa et al.*, 1997]. P1 subsequently returns to the magnetosheath, and then crosses fully into stagnant plasma at just before 18:50 UT.

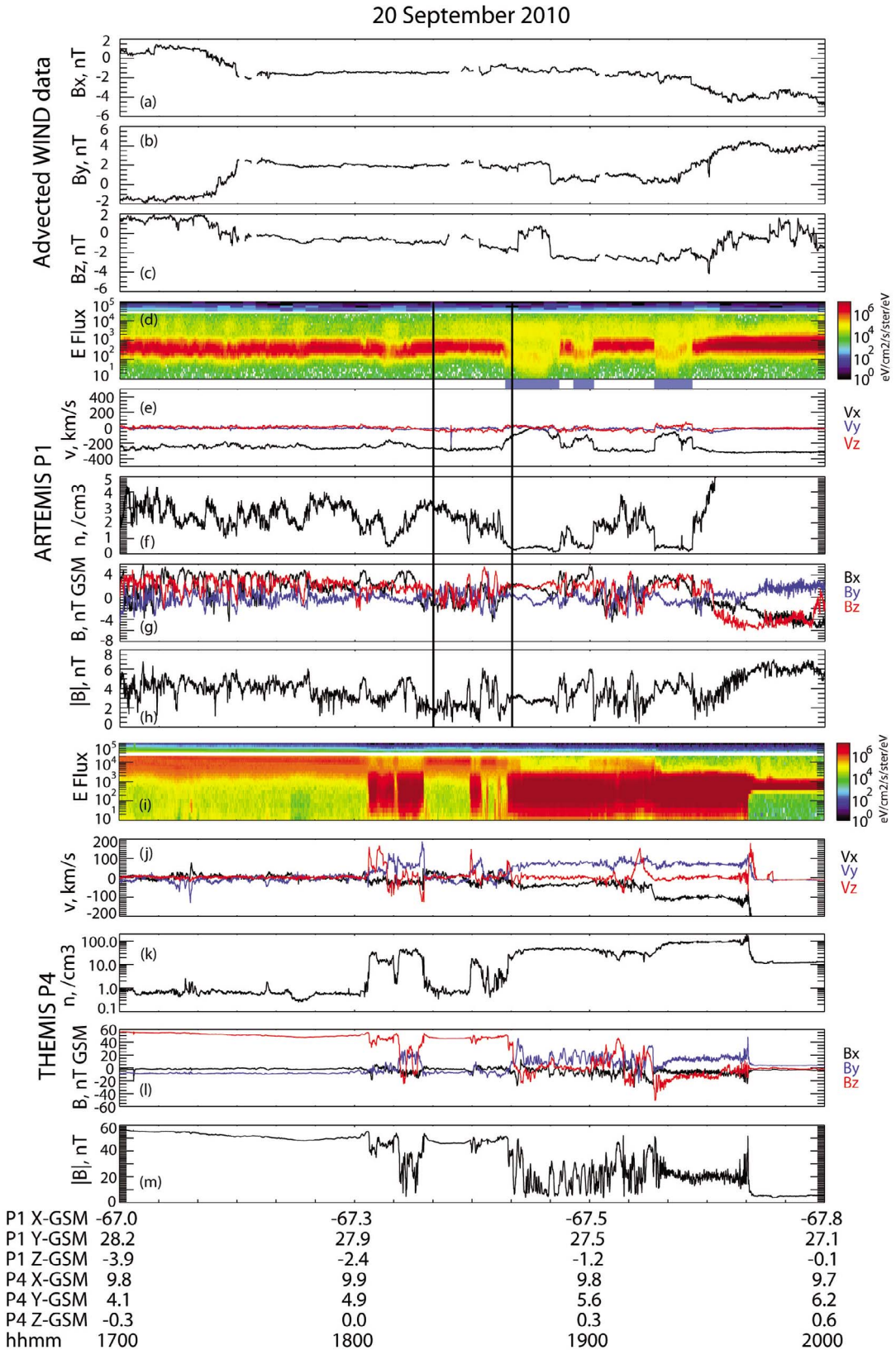

Figure 2. (a–c) Wind measurements of the B_X, B_Y, B_Z components of the IMF in the GSM coordinate system, lagged by 87 min. (d–h) ARTEMIS P1 ion energy flux spectrogram, ion velocity, ion density, magnetic field components and magnetic field strength. (i–m) THEMIS P4 ion energy flux spectrogram, ion velocity, ion density, magnetic field components and magnetic field strength. Vectors are presented using the GSM coordinate system.

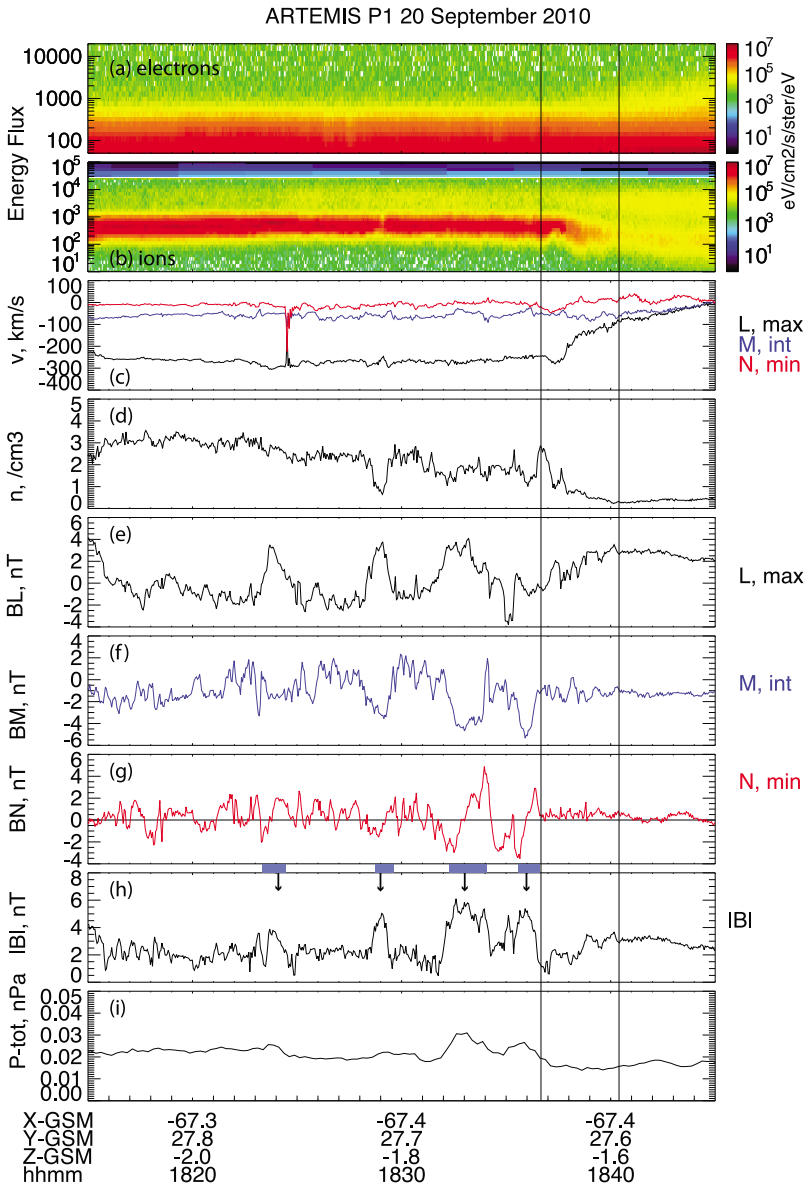

Figure 3. (a, b) ARTEMIS-P1 electron and ion energy flux spectrograms, (c, d) ion velocity and density, (e–h) magnetic field components and strength, and (i) total ion pressure. FTEs are identified by vertical arrows. Data are shown in a local boundary normal coordinate system.

[10] The interval 18:20–18:40 UT, just prior to the first of these magnetopause encounters, is shown in more detail in Figure 3. The data have been transformed into a local boundary coordinate system [**L**, **M**, **N**] where **L** contains the main magnetic field reversal and **N** is the boundary normal. This coordinate system is derived from minimum variance analysis of the current sheet crossing between 18:36:40 UT–18:40:24 UT, with the maximum, intermediate and minimum variance directions corresponding to **L**, **M** and **N** respectively. Here **L** = (0.948, −0.017, 0.319), **M** = (0.319, 0.101, −0.942) and **N** = (−0.016, 0.995, 0.102), with eigenvalues $\{\lambda_1 = 1.31, \lambda_2 = 0.27, \lambda_3 = 0.10\}$. As expected from the location of P1 shown in Figure 1, the local magnetopause normal points in the $+y_{GSM}$ direction. Note that magnetic field draping changes $+B_y$ in the subsolar magnetosheath to $-B_L$ (i.e., $-B_x$) in the flank magnetosheath. The magnetic field points Earthward in the magnetosphere ($B_L > 0$). The overall geometry is discussed in more detail in section 5.

[11] P1 observed four enhancements in the magnetic field strength (marked by vertical arrows in Figure 3h), accompanied by in/out (−, +) perturbations in B_N, the component of the magnetic field normal to the magnetopause at 18:24 UT, 18:29 UT, 18:33 UT and 18:36 UT. Although the density is reduced in some events (e.g., #2), the total pressure increases inside each event (particularly in #3). Based on these characteristics, these features are identified as flux transfer events. If they were due to boundary fluctuations caused by the Kelvin-Helmholtz instability, then this would induce a vorticity i.e., a significant perturbation in v_N [*Hasegawa et al.*, 2004] which is not observed.

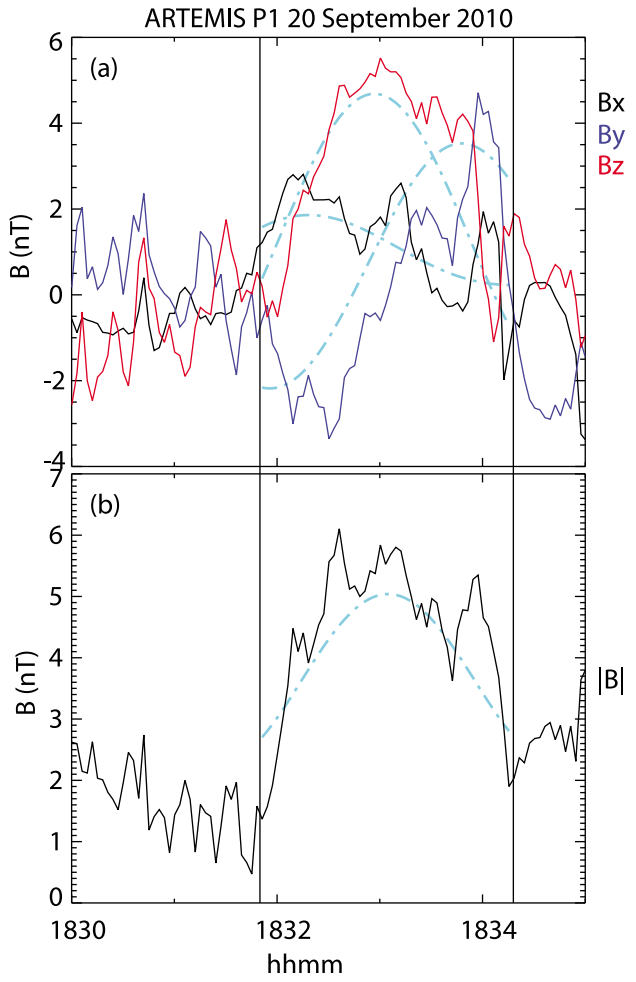

Figure 4. (a, b) ARTEMIS-P1 observations of FTE #3 and the best fit to a force free flux rope model.

[12] In order to determine their properties more quantitatively, a force-free flux rope model (i.e., $\mathbf{J} \times \mathbf{B} = 0$) whose solution is a cylindrically symmetric helical magnetic field: $B_z(r) = B_0 J_0(\alpha r)$, $B_\theta(r) = B_0 H J_1(\alpha r)$, $B_r = 0$ (B_0 = peak core magnetic field, α = constant, H = handedness, Bessel function J_ν) was applied to each structure [*Burlaga*, 1988; *Lepping et al.*, 1990, and references therein]. It is assumed that the satellite follows a straight-line trajectory through the rope, which is defined by the impact factor (the closest approach to the flux rope axis). The interval is first transformed using MVA and the intermediate variance direction, containing a unipolar variation in the magnetic field, is identified as the axis of the flux rope without further optimization [e.g., *Lepping et al.*, 1990]. A least squares fit is then performed between the data and the model, varying the model core field and the model impact parameter. We note however that MVA would not necessarily work if the flux rope was not force free [*Xiao et al.*, 2004].

[13] This model was applied to each of the four FTEs. Excellent fits to the force free model were recovered for #3 and #4. Figure 4 shows flux rope #3 together with the best fit to the force-free model (note the data are shown in the GSM coordinate system). The axis of flux rope #3 is calculated to be $\mathbf{n} = [-0.514, -0.094, 0.853]$, with an impact factor $Y_0 = 0.05$ ($Y_0 = 0$ is the center of the flux rope whereas at $Y_0 = 1$, the magnetic field is perpendicular to the flux rope axis). The model core field is $B_0 = 5.1$ nT. The fit to flux rope #4 is shown in the same format in Figure 5. Here, the axis is calculated to be $\mathbf{n} = [-0.169, 0.222, 0.960]$. In this case, $Y_0 = 0.35$, indicating that the satellite did not pass as close to the axis of the flux rope. As such, although the observed peak field in #4 is slightly less than that observed in #3, the model core field $B_0 = 5.5$ nT for flux rope #4. In both cases, the flux ropes have positive (right) handedness.

[14] Relatively poor fits to #1 and #2 were found, possibly because the satellite, being slightly further from the magnetopause, did not pass close enough to the center of the flux rope [*Rees*, 2002]. If a satellite encounters the draped fields around the FTE, rather than the core of the FTE itself, then the minimum variance direction should be identified as the FTE axis [*Farrugia et al.*, 1987]. For FTE #1, the minimum variance direction is found to be $\mathbf{n} = [-0.608, -0.285, 0.740]$ ($\lambda_2/\lambda_3 = 11.6$), and for FTE #2, $\mathbf{n} = [-0.721, -0.390, 0.573]$ ($\lambda_2/\lambda_3 = 5.0$).

[15] Given the consistency in the orientations of the four FTE axes (all pointing in the −x/+z direction), it therefore appears that P1 encountered the first two FTEs further away from the magnetopause, and observed draped field signatures, whereas it encountered the core regions of the third

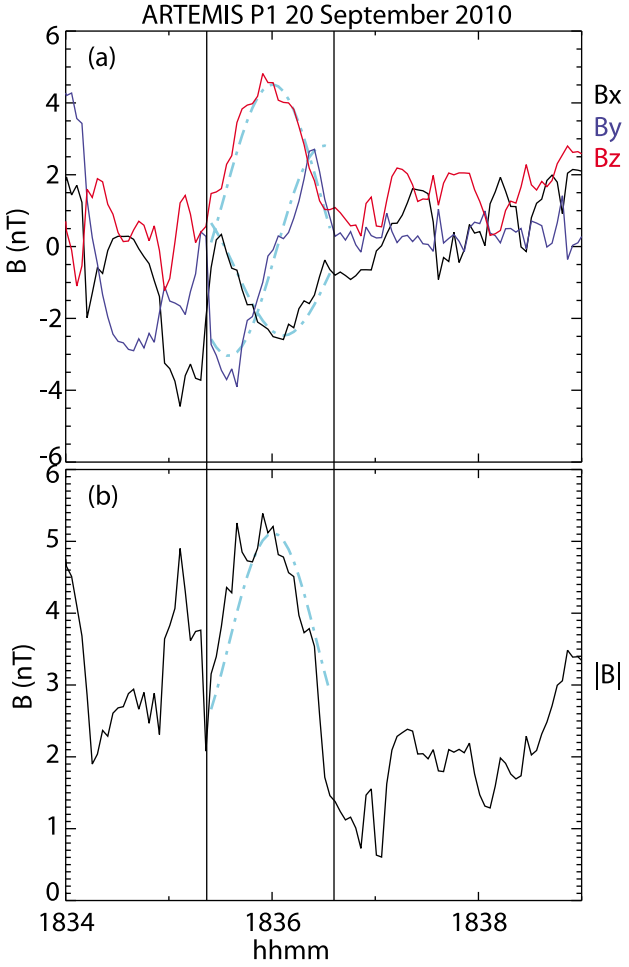

Figure 5. (a, b) ARTEMIS-P1 observations of FTE #4 and the best fit to a force free flux rope model.

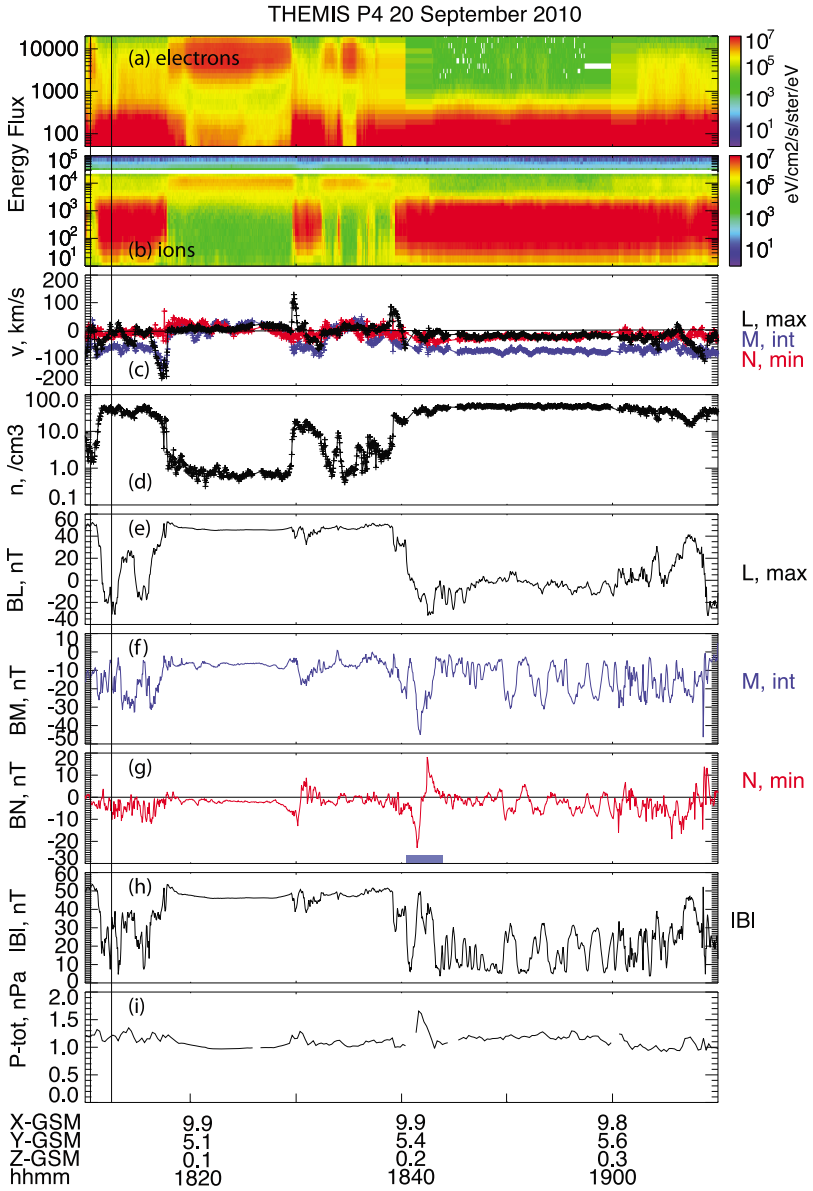

Figure 6. (a, b) THEMIS-P4 electron and ion energy flux spectrograms, (c, d) ion velocity and density, (e–h) magnetic field components and strength, and (i) total ion pressure. Data are shown in a local boundary normal coordinate system.

and fourth FTEs. This is also consistent with the overall trajectory of P1 being directed from the magnetosheath to the magnetosphere.

[16] It is expected that the flux ropes should lie parallel to the plane of the local magnetopause, and so a simple consistency check can be made by calculating the angle between each flux rope axis and the current sheet normal. The angles between the four flux rope axes and the current sheet normal are 101°, 109°, 90° and 97° respectively, confirming that the structures lie parallel to the plane of the local magnetopause.

4. THEMIS P4 Subsolar Magnetopause Observations

[17] During the interval shown in Figure 2, P4 was on the outbound leg of its orbit and crossed the magnetopause several times between 18:00 UT–19:00 UT. Similar observations were made by THEMIS P3 and P5 located nearby. The data are shown in Figure 6, again transformed into a local boundary normal coordinate system based on the magnetopause crossing that occurred between 18:10:30 UT–18:12:30 UT. As before, [**L**, **M**, **N**] correspond to the maximum, intermediate and minimum variance directions with **L** = (0.029, −0.288, 0.957), **M** = (0.164, −0.943, −0.289) and **N** = (0.986, 0.165, 0.021). The corresponding eigenvalues are $\{\lambda_1 = 875.7, \lambda_2 = 33.3, \lambda_3 = 4.74\}$. The magnetosheath flow itself is predominantly in the −**M** (duskward) direction, as expected given that P4 is duskward (y > 0) of the subsolar point. At several of the magnetopause crossings, plasma jets perpendicular to the current sheet normal are observed. This is indicative of ongoing magnetopause reconnection [*Phan et al.*, 2000]; for example at 18:17 UT a

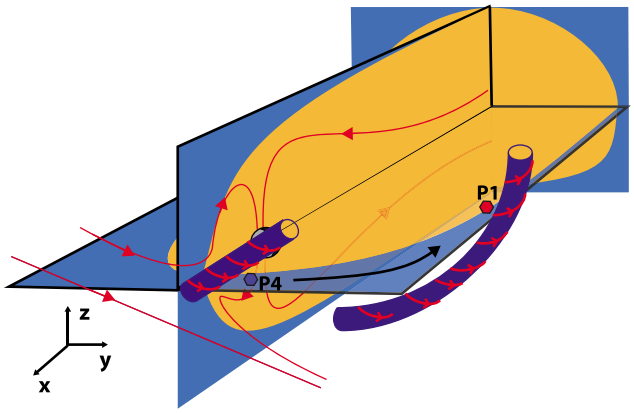

Figure 7. Cartoon showing the transport of an FTE flux rope from the dayside magnetopause to the dusk flank tail magnetopause in a manner consistent with observations, under conditions of IMF $B_y > 0$ and $B_z < 0$.

jet in the $-\mathbf{L}/-\mathbf{M}$ direction is observed (i.e., southward and duskward). At 18:30 UT a jet ($v_L \sim 130$ km s^{-1}) in the $+\mathbf{L}$ direction is observed, reversing to the $-\mathbf{L}$ direction at 18:32 UT. The reversal in the jet direction suggests that the satellite is in the vicinity of an X-line. Similarly there is a reversal in v_L from positive to negative at 18:40 UT (although note that there is a short data gap in the ion plasma data between 18:40:24 UT–18:41:16 UT).

[18] In addition to plasma jets, several bipolar perturbations to the normal magnetic field, indicative of FTEs, were observed. For example, there is an in/out (−, +) perturbation in B_N between 18:41:00 UT–18:43:30 UT, which occurs for negative v_L and negative v_M (although there is a data gap as noted above). This negative/positive perturbation is consistent with a southward moving FTE. A good fit to the force free model could not be obtained; this appears to be due to the double-peak structure in the total field. However, there is a negative enhancement in the B_M component of the field in the FTE, which indicates that the axial field of the FTE points duskward and northward. Consequently, this flux rope has positive (right) handedness. Signatures of active multiple X-line FTE formation such as converging flows reversing across the FTE or bi-directional electrons on the magnetosheath side [*Hasegawa et al.*, 2010; *Øieroset et al.*, 2011] were not captured in this event, which is not unusual given their rarity in the data [*Zhang et al.*, 2012]. Other FTEs were also observed, for example at 18:05 UT and 19:08 UT. While this flux rope is evidently not the one of those observed on the flank by ARTEMIS, it does indicate that under the prevailing solar wind conditions, FTEs were being produced on the dayside magnetosphere.

5. Discussion

[19] The observations made by P1 are most consistent with the passage of FTEs carrying a helical flux rope magnetic field structure. It is unlikely that these flux ropes are generated locally on the tail flank magnetopause, since the flow shear between the magnetosheath and magnetosphere is very large: $v_L \sim 280$ km s^{-1}, whereas the Alfvén speed in the magnetosheath is ~30 km s^{-1} (given $|\mathbf{B}| = 2$ nT and $n = 2$ cm^{-3}). This is expected to suppress the local onset of reconnection [*La Belle-Hamer et al.*, 1995; *Cassak*, 2011].

[20] It is worth noting that the flow shear is less between the mantle and the magnetosheath, and therefore it may be possible to imagine a scenario whereby reconnection could occur on the tail flank closer to P1. The appearance of the plasma sheet just next to the magnetopause (at ~18:40 UT) could be linked to the erosion of mantle field lines through reconnection between the mantle and magnetosheath, which led to the creation of the flux ropes. However, in the case at hand, the flow speed in the mantle observed just prior to the FTEs at 18:14 UT was of the order of $v_L \sim 200$ km s^{-1}, and so the velocity shear still exceeds the Alfvén speed. Furthermore, reconnection can be suppressed if the jump in the plasma beta exceeds some critical parameter based on the magnetic shear [*Swisdak et al.*, 2003, 2010 equation 3]. Evidence for this mechanism has been observed at reconnecting solar wind current sheets and Saturn's magnetopause [*Phan et al.*, 2010; *Masters et al.*, 2012], and so it is reasonable to assume it is also relevant here. In this event, the change in the plasma beta is ~12.3 since $\beta_{\text{magnetosheath}} \sim 16$ ($\langle n \rangle \sim 2.8$ cm^{-3}, $\langle T \rangle \sim 0.5$ MK and $\langle B \rangle \sim 1.7$ nT) and $\beta_{\text{plasma sheet}} \sim 3.7$ ($\langle n \rangle \sim 0.4$ cm^{-3}, $\langle T \rangle \sim 2.7$ MK and $\langle B \rangle \sim 3$ nT). The magnetic shear is 148°, thus suggesting that magnetic reconnection is suppressed. We therefore consider how the observations may fit with FTE dynamics on the dayside magnetopause.

[21] At the dayside magnetopause, the incident solar wind magnetic field pointed southward and duskward (B_y positive, and $|B_y| > |B_z|$). Under IMF conditions that are southward with a dawn-dusk component, recent Cluster/THEMIS/Double-Star observations indicate that a component reconnection X-line can form, extending across the dayside magnetopause [*Dunlop et al.*, 2011a, 2011b]. In a recent modeling study, it has been shown that under these conditions, such component reconnection along an extended X-line can result in flux ropes whose axes point in the +y, +z direction, where the core magnetic field, defined by the guide field, points along the axis [*Sibeck and Lin*, 2011]. This is illustrated in Figure 7. Note that if B_y is positive, the resultant flux ropes have positive handedness. If the flux rope is generated by multiple X-line reconnection and moves southward, it will move toward the dusk flank, generating an in/out (−, +) B_n perturbation as shown in Figure 7. This is consistent with the THEMIS P4 observations.

[22] As the flux rope convects anti-sunward and duskward on the magnetopause, the model shows that the flux rope will occupy the +y/−z quadrant of the magnetopause [*Sibeck and Lin*, 2011]. This model therefore predicts that flux ropes observed on the dusk flank under such IMF conditions should have a positive handedness and a −/+ normal magnetic field perturbation, all of which is consistent with the observations made by ARTEMIS P1. The model predicts that the FTE can have a significant curvature on the flanks, with the part of the FTE below the ecliptic oriented north-south, (as seen by ARTEMIS P1 at $z_{GSM} < 0$) but near the ecliptic the FTE is more confined to the ecliptic plane. We note that if they were formed in the manner originally proposed by *Russell and Elphic* [1978], one might expect the axis to be more aligned to the Sun-Earth line, perpendicular to the observed orientation [*Sibeck and Siscoe*, 1984]. FTEs which have axial orientations that are perpendicular to the

prediction of *Russell and Elphic* [1978] and closer to that expected of extended X-line models have also been reported in the subsolar region [*Fear et al.*, 2012]. Figure 7 shows the North-South orientation of the FTE at ARTEMIS P1, and its possible extension toward the polar tail magnetopause.

[23] It is of interest to consider how the flux rope FTEs evolve as they move from the subsolar to the distant tail magnetopause. First, if the observed flux-rope FTEs are sourced from the dayside magnetosphere, this indicates that they remain coherent for a long time, since the transport time from the dayside magnetopause to the observation point is of the order of 30 min. They must therefore achieve a state of quasi-equilibrium which is consistent with the observations of internal structure reaching a force-free configuration.

[24] At P1, if it is assumed that they are moving at the magnetosheath flow speed (approximately 280 km s^{-1}), the duration of each event (56 s, 50 s, 148 s and 74 s respectively) leads to an estimated size of 2.5 R_E, 2.2 R_E, 6.5 R_E, and 3.3 R_E. In the two cases where a good fit to the force free model was obtained, the impact factors were small indicating that these sizes essentially correspond to the flux rope diameter. From this, we can calculate the flux content. It can be shown that for a force-free flux rope, the flux content Φ is given by

$$\Phi = 0.4158\left[2\pi B_0 R_f^2 J_1(2.40482)\right] \quad (1)$$

where B_0 is the core field strength, R_f is the flux rope radius and J_1 is a Bessel function. For flux ropes #3 and #4, the total flux is estimated to be 2.96 MWb and 0.80 MWb respectively. These values are comparable to previous estimates of flux content in FTEs at Earth on the dayside magnetopause [*Rijnbeek et al.*, 1984; *Hasegawa et al.*, 2006].

[25] At THEMIS P4, the flow speed parallel to the magnetopause associated with the FTE discussed in the previous section is ~80 km s^{-1}. If it assumed that this corresponds to the speed with which the FTE is moving, then the duration of approximately 2 min corresponds to a scale size of ~1.5 Re. Even though a good fit to the force free model was not recovered, a rough estimate of the flux content can be calculated as $\varphi = \pi\langle B_0\rangle R_f^2 = 1.43$ MWb given $R_f \sim 0.75$ Re and the mean magnetic field $\langle B_0\rangle \sim 20$ nT. As such, it would appear that although the FTEs may grow in size, perhaps by a factor of 2–4 due to the reduction in the ambient magnetosheath pressure, the flux content does not seem to change considerably. Although these observations demonstrate qualitatively the existence of flux ropes FTEs far downtail, quantitative results concerning changes in size and flux content require many more such FTEs to be observed so that statistics can be constructed.

[26] Finally, we briefly consider the connectivity of the flux ropes. Unfortunately, we are unable to determine this using electron distributions since P1 was in slow survey mode and no fast 3d electron distributions were captured inside any of the flux rope events, precluding analysis of field aligned electron beams. However, the boundary layer observed inside the magnetopause after the passage of the FTEs consisted of a two component ion population (i.e., containing cold plasma) on closed field lines, indicated by bi-directional electron beams. This boundary layer presumably formed during the previous northward IMF interval [e.g., *Øieroset et al.*, 2005], but was observed after the FTEs were encountered, and so was not destroyed by their passage. Given that the modeling indicates P1 passed close to the center of the flux ropes while in the magnetosheath flow, this perhaps tentatively suggests that the flux ropes were not closed into the magnetosphere at both ends. However, if reconnection occurs in an asymmetric current layer, the center of the FTE bulge is displaced toward the magnetosheath [e.g., *Scholer*, 1989]. Alternatively, if they are indeed closed into the magnetosphere at both ends, it would therefore appear that the flux ropes had not yet been entrained across the magnetopause into the magnetotail plasma, even at -67 R_E downtail.

6. Conclusions

[27] Novel data from ARTEMIS has led to the discovery of FTEs far along the tail magnetopause. A very good fit to a force free flux rope model was found for the two FTEs observed closest to the tail flank magnetopause. Given the large velocity shear across the magnetopause, it is unlikely that they are created locally. Simultaneous observations from THEMIS on the dayside magnetopause show the presence of reconnection jets and FTEs. The FTE size at ARTEMIS is 2–4 times greater than that observed on the dayside magnetopause, but the flux content is comparable to FTEs observed on the dayside magnetopause. The magnetosheath convection time indicates that they must have a long lifetime in order for them to survive far downtail, which is consistent with them having reached a state of quasi-equilibrium. The handedness and perturbations generated by the FTEs at ARTEMIS can be explained by considering the expected motion of flux rope FTEs generated by an extended X-line on the dayside magnetopause in the presence of a dawn-dusk IMF field component.

[28] In the present case it is not possible to reach a definitive conclusion as to whether the FTEs at ARTEMIS are open or closed. Indeed it is likely that in general, FTEs are not homogenous, and contain some fraction of open, closed and disconnected field (relative to the Earth). If FTEs do have a completely (or mainly) disconnected magnetic field structure, then their role in solar wind-magnetosphere coupling requires re-assessment, since the FTE itself would not transport flux into the magnetotail. Other data from ARTEMIS, together with simulations, should be examined to determine the statistical properties of flux ropes on the tail magnetopause (particularly size, topology, geometry and flux content), leading to an improved understanding of their ultimate fate and role in plasma transport across the magnetopause.

[29] **Acknowledgments.** J.P.E. holds an STFC Advanced Fellowship at ICL. We acknowledge NASA contract NAS5–02099 for use of data from the THEMIS Mission, specifically D. Larson and R. P. Lin for use of SST data; C. W. Carlson and J. P. McFadden for use of ESA data; and K. H. Glassmeier, U. Auster, and W. Baumjohann for the use of FGM data provided under the lead of the Technical University of Braunschweig and with financial support through the German Ministry for Economy and Technology and the German Center for Aviation and Space (DLR) under contract 50 OC 0302.

[30] Philippa Browning thanks the reviewers for their assistance in evaluating the paper.

References

Angelopoulos, V. (2008), The THEMIS mission, *Space Sci. Rev.*, *141*, 5–34, doi:10.1007/s11214-008-9336-1.

Angelopoulos, V. (2011), The ARTEMIS mission, *Space Sci. Rev.*, *165*, 3–25, doi:10.1007/s11214-010-9687-2.

Burlaga, L. F. (1988), Magnetic clouds and force-free fields with constant alpha, *J. Geophys. Res.*, *93*, 7217–7224, doi:10.1029/JA093iA07p07217.

Cassak, P. A. (2011), Theory and simulations of the scaling of magnetic reconnection with symmetric shear flow, *Phys. Plasmas*, *18*, 072106, doi:10.1063/1.3602859.

Dungey, J. W. (1961), Interplanetary magnetic field and the auroral zones, *Phys. Rev. Lett.*, *6*, 47–48, doi:10.1103/PhysRevLett.6.47.

Dunlop, M. W., et al. (2011a), Extended magnetic reconnection across the dayside magnetopause, *Phys. Rev. Lett.*, *107*, 025004, doi:10.1103/PhysRevLett.107.025004.

Dunlop, M. W., et al. (2011b), Magnetopause reconnection across wide local time, *Ann. Geophys.*, *29*, 1683–1697, doi:10.5194/angeo-29-1683-2011.

Fairfield, D. H., and L. J. Cahill (1966), Transition region magnetic field and polar magnetic disturbances, *J. Geophys. Res.*, *71*, 155–169, doi:10.1029/JZ071i001p00155.

Farris, M. H., S. M. Petrinec, and C. T. Russell (1991), The Thickness of the Magnetosheath: Constraints on the Polytropic Index, *Geophys. Res. Lett.*, *18*(10), 1821–1824, doi:10.1029/91GL02090.

Farrugia, C. J., R. C. Elphic, D. J. Southwood, and S. W. H. Cowley (1987), Field and flow perturbations outside the reconnected field line region in flux transfer events, *Planet. Space Sci.*, *35*, 227–240, doi:10.1016/0032-0633(87)90091-2.

Fear, R. C., A. N. Fazakerley, C. J. Owen, and E. A. Lucek (2005), A survey of flux transfer events observed by Cluster during strongly northward IMF, *Geophys. Res. Lett.*, *32*, L18105, doi:10.1029/2005GL023811.

Fear, R. C., S. E. Milan, A. N. Fazakerley, E. A. Lucek, S. W. H. Cowley, and I. Dandouras (2008), The azimuthal extent of three flux transfer events, *Ann. Geophys.*, *26*, 2353–2369, doi:10.5194/angeo-26-2353-2008.

Fear, R. C., S. E. Milan, and K. Oksavik (2012), Determining the axial direction of high-shear flux transfer events: Implications for models of FTE structure, *J. Geophys. Res.*, doi:10.1029/2012JA017831, in press.

Hasegawa, H., K. Maezawa, T. Mukai, and Y. Saito (2002a), Plasma entry across the distant tail magnetopause 1. Global properties and IMF dependence, *J. Geophys. Res.*, *107*(A5), 1063, doi:10.1029/2001JA900139.

Hasegawa, H., K. Maezawa, T. Mukai, and Y. Saito (2002b), Plasma entry across the distant tail magnetopause 2. Comparison between MHD theory and observation, *J. Geophys. Res.*, *107*(A6), 1073, doi:10.1029/2001JA900138.

Hasegawa, H., M. Fujimoto, T.-D. Phan, H. Rème, A. Balogh, M. W. Dunlop, C. Hashimoto and R. TanDokoro (2004), Transport of solar wind into Earth's magnetosphere through rolled-up Kelvin-Helmholtz vortices, *Nature*, *430*, 755–758, doi:10.1038/nature02799.

Hasegawa, H., B. U. Ö. Sonnerup, C. J. Owen, B. Klecker, G. Paschmann, A. Balogh, and H. Rème (2006), The structure of flux transfer events recovered from Cluster data, *Ann. Geophys.*, *24*, 603–618, doi:10.5194/angeo-24-603-2006.

Hasegawa, H., et al. (2010), Evidence for a flux transfer event generated by multiple X-line reconnection at the magnetopause, *Geophys. Res. Lett.*, *37*, L16101, doi:10.1029/2010GL044219.

Kawano, H., and C. T. Russell (1997), Survey of flux transfer events observed with the ISEE 1 spacecraft: Dependence on the interplanetary magnetic field, *J. Geophys. Res.*, *102*, 11,307–11,313, doi:10.1029/97JA00481.

La Belle-Hamer, A. L., A. Otto, and L. C. Lee (1995), Magnetic reconnection in the presence of sheared flow and density asymmetry: Applications to the Earth's magnetopause, *J. Geophys. Res.*, *100*, 11,875–11,889.

Lee, L. C., and Z. F. Fu (1985), A theory of magnetic flux transfer at the Earth's magnetopause, *Geophys. Res. Lett.*, *12*, 105–108, doi:10.1029/GL012i002p00105.

Lepping, R. P., J. A. Jones, and L. F. Burlaga (1990), Magnetic field structure of interplanetary magnetic clouds at 1 AU, *J. Geophys. Res.*, *95*, 11,957–11,965, doi:10.1029/JA095iA08p11957.

Maezawa, K., T. Hori, T. Mukai, Y. Saito, T. Yamamoto, S. Kokubun, and A. Nishida (1997), Structure of the distant magnetotail and its dependence on the IMF By component: Geotail observations, *Adv. Space Res.*, *20*, 949–959, doi:10.1016/S0273-1177(97)00503-6.

Masters, A., J. P. Eastwood, M. Swisdak, M. F. Thomsen, C. T. Russell, N. Sergis, F. J. Crary, M. K. Dougherty, A. J. Coates, and S. M. Krimigis (2012), The importance of plasma β conditions for magnetic reconnection at Saturn's magnetopause, *Geophys. Res. Lett.*, *39*, L08103, doi:10.1029/2012GL051372.

Øieroset, M., J. Raeder, T.-D. Phan, S. Wing, J. P. McFadden, W. Li, M. Fujimoto, H. Reme, and A. Balogh (2005), Global cooling and densification of the plasma sheet during an extended period of purely northward IMF on October 22–24, 2003, *Geophys. Res. Lett.*, *32*, L12S07, doi:10.1029/2004GL021523.

Øieroset, M., et al. (2011), Direct evidence for a three-dimensional magnetic flux rope flanked by two active magnetic reconnection X lines at Earth's magnetopause, *Phys. Rev. Lett.*, *107*, 165007, doi:10.1103/PhysRevLett.107.165007.

Omidi, N., and D. G. Sibeck (2007), Flux transfer events in the cusp, *Geophys. Res. Lett.*, *34*, L04106, doi:10.1029/2006GL028698.

Phan, T. D., et al. (2000), Extended magnetic reconnection at the Earth's magnetopause from detection of bi-directional jets, *Nature*, *404*, 848–850, doi:10.1038/35009050.

Phan, T.-D., et al. (2010), The dependence of magnetic reconnection on plasma β and magnetic shear: Evidence from solar wind observations, *Astrophys. J.*, *719*, L199–L203, doi:10.1088/2041-8205/719/2/L199.

Raeder, J. (2006), Flux transfer events: 1. Generation mechanism for strong southward IMF, *Ann. Geophys.*, *24*, 381–392, doi:10.5194/angeo-24-381-2006.

Rees, A. (2002), Ulysses observations of magnetic clouds in the 3-D heliosphere, PhD thesis, Imp. Coll. of Sci. Technol. and Med., Univ. of London, London.

Rijnbeek, R. P., S. W. H. Cowley, D. J. Southwood, and C. T. Russell (1984), A survey of dayside flux transfer events observed by ISEE 1 and 2 magnetometers, *J. Geophys. Res.*, *89*, 786–800, doi:10.1029/JA089iA02p00786.

Russell, C. T., and R. C. Elphic (1978), Initial ISEE magnetometer results: Magnetopause observations, *Space Sci. Rev.*, *22*, 681–715, doi:10.1007/BF00212619.

Scholer, M. (1988), Magnetic flux transfer at the magnetopause based on single X-line bursty reconnection, *Geophys. Res. Lett.*, *15*, 291–294, doi:10.1029/GL015i004p00291.

Scholer, M. (1989), Asymmetric time-dependent and stationary magnetic reconnection at the dayside magnetopause, *J. Geophys. Res.*, *94*, 15,099–15,111, doi:10.1029/JA094iA11p15099.

Sibeck, D. G., and R.-Q. Lin (2011), Concerning the motion and orientation of flux transfer events produced by component and antiparallel reconnection, *J. Geophys. Res.*, *116*, A07206, doi:10.1029/2011JA016560.

Sibeck, D. G., and G. L. Siscoe (1984), Downstream properties of magnetic flux transfer events, *J. Geophys. Res.*, *89*(A12), 10,709–10,715, doi:10.1029/JA089iA12p10709.

Sibeck, D. G., et al. (2011), ARTEMIS Science Objectives, *Space Sci. Rev.*, *165*, 59–91, doi:10.1007/s11214-011-9777-9.

Southwood, D. J., C. J. Farrugia, and M. A. Saunders (1988), What are flux transfer events?, *Planet. Space Sci.*, *36*, 503–508, doi:10.1016/0032-0633(88)90109-2.

Swisdak, M., B. N. Rogers, J. F. Drake, and M. A. Shay (2003), Diamagnetic suppression of component magnetic reconnection at the magnetopause, *J. Geophys. Res.*, *108*(A5), 1218, doi:10.1029/2002JA009726.

Swisdak, M., et al. (2010), The vector direction of the interstellar magnetic field outside the heliosphere, *Astrophys. J.*, *710*, 1769–1775, doi:10.1088/0004-637X/710/2/1769.

Wang, Y. L., R. C. Elphic, B. Lavraud, M. G. G. T. Taylor, J. Birn, C. T. Russell, J. Raeder, H. Kawano, and X. X. Zhang (2006), Dependence of flux transfer events on solar wind conditions from 3 years of Cluster observations, *J. Geophys. Res.*, *111*, A04224, doi:10.1029/2005JA011342.

Xiao, C. J., Z. Y. Pu, Z. W. Ma, S. Y. Fu, Z. Y. Huang, and Q.-G. Zong (2004), Inferring of flux rope orientation with the minimum variance analysis technique, *J. Geophys. Res.*, *109*, A11218, doi:10.1029/2004JA010594.

Zhang, H., M. G. Kivelson, V. Angelopoulos, K. K. Khurana, Z. Y. Pu, R. J. Walker, R. L. McPherron, T.-S. Hsu, Q. G. Zong, and T. Phan (2012), Generation and properties of in vivo flux transfer events, *J. Geophys. Res.*, *117*, A05224, doi:10.1029/2011JA017166.